AD-A151 748   A SCANNING OPTICAL MICROPROBE FOR INFRARED DETECTOR MEASUREMENT(U) ROYAL SIGNALS AND RADAR ESTABLISHMENT MALVERN (ENGLAND) H A TARRY 1984 RSRE-MEMO-3745   1/1

UNCLASSIFIED   DRIC-BR-94725   F/G 17/5   NL

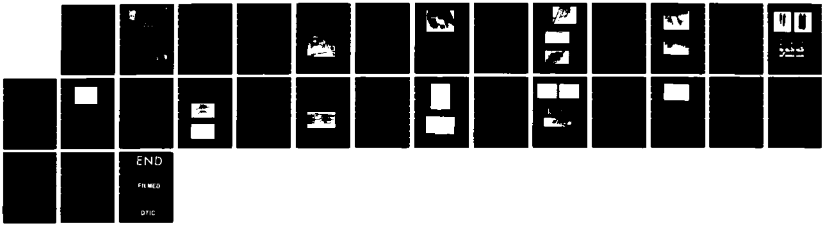

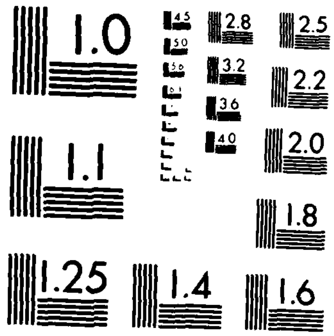

MICROCOPY RESOLUTION TEST CHART
NATIONAL BUREAU OF STANDARDS-1963-A

UNLIMITED

RSRE MEMORANDUM No. 3745

ROYAL SIGNALS & RADAR ESTABLISHMENT

A SCANNING OPTICAL MICROPROBE FOR INFRARED DETECTOR MEASUREMENT

Author: H A Tarry

PROCUREMENT EXECUTIVE,
MINISTRY OF DEFENCE,
RSRE MALVERN,
WORCS.

UNLIMITED

ROYAL SIGNALS AND RADAR ESTABLISHMENT

Memorandum 3745

Title: A Scanning Optical Microprobe for Infrared Detector Measurement.

Author: H A Tarry

Date:

SUMMARY

An optical probe apparatus is described which has been used for mapping the responsivity and defects of a range of IR detectors and has been extended to measure minority carrier lifetime, ambipolar mobility, photo-luminescence and diffusion length. Each use of the apparatus is illustrated with experimental results.

A SCANNING OPTICAL MICROPROBE FOR INFRARED DETECTOR MEASUREMENTS

H A TARRY

1. INTRODUCTION

Long wavelength infrared detectors have dimensions typically measured in tens of microns. It is important to be able to measure variations in detector properties within this area, both to ensure that there are no 'dead' parts which could fail to detect a small area of irradiance, and as a guide to defects in the material and manufacture which could reduce the detectivity of the whole area.

This memorandum describes an optical microprobe apparatus which was designed to carry out these measurements by mapping the photoconductive or photovoltaic properties of a director on a microscopic scale with a resolution of a few microns (or better). The first sections describe the construction and use of the apparatus for this purpose, and later sections are accounts of the extension of the apparatus to measure a range of other properties of detectors and semiconductor material, in particular diffusion length, minority carrier lifetime, mobility and photoluminescence.

Each use of the apparatus is illustrated with examples selected to show the wide range of measurements that can be done and conclusions that can be drawn from them, but the detailed use in each case may be reported separately.

2. DESIGN AND CONSTRUCTION

All the measurements described in this memo rely on an ability to move a small focussed spot of radiation in a controlled manner (eg a raster) over the surface of a small sample. Figure 1 shows how this was done: a microscope (e) was used in reverse to focus a beam of parallel light (eg. a laser, (a)) on to the sample (f); since the position of the spot depends on the angle of light entering the microscope eyepiece, a galvanometer

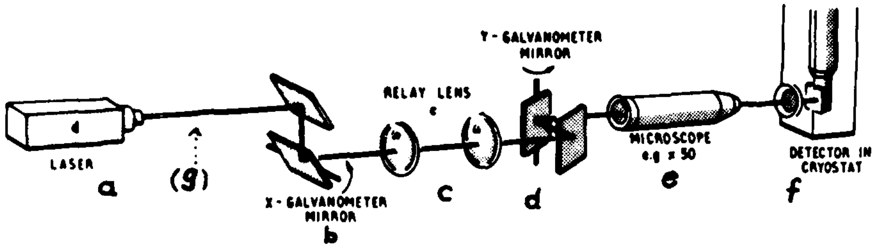

Figure 1

Diagram of the optical layout of the apparatus

Figure 2

The probe apparatus set up for lifetime measurement using the CF204 cryostat

mirror (d) turning at the eyepiece pupil gives the necessary linear motion to the spot. If the eyepiece pupil is filled by the beam the microscope is working inversely to its designed use and lens aberrations, resolution and distortion are at a minimum. Moving the spot at right angles is done by a second galvanometer (b) at an optically equivalent position set by the relay lens (c). This is a pair of lenses separated by the sum of their focal lengths. The galvanometers were made by General Scanning Inc. and give a controlled angular deflection proportional to the input voltage at their driver amplifiers at frequencies up to $1kH_z$. Provided the deflection is not too large for the microscope eyepiece to accommodate, distortion of a square raster on the specimen is less than 1%.

The small optical items were mounted on a heavy optical bench capable of supporting additional lasers at (g) and a cryostat for the sample at (f). Most of the measurements reported here were on IR detectors and required temperatures below 200K, and cooling was done either in a simple side-window cryostat (1) cooled by refringerant gases such as Freons or liquid N_2, or in an Oxford Instruments CF204 cryostat (4K to 300K) mounted on a positioner (and weighing 25kg).

Drive signals for the galvanometers were produced by a scan generator designed by JJ Low of RSRE (Baldock) and several have been built by MESD at RSRE. It enables the light spot to be moved in a controlled and variable raster of up to 511 lines and has the facilities of variable raster size, raster rotation, single line scanning etc. Slaved to the raster is the spot on a CRT (in a similar way to the SEM) and its position or intensity can be modulated by the response of the sample to the light spot. An XY recorder can also be used to record the map. Fugure 2 shows the completed apparatus with the CF204 cryostat in position. Most of the electronic apparatus shown here is associated with lifetime measurement. (Section 4 below)

When first setting up the apparatus care was taken that all the optical items were positioned so that further items could be added without realignment e.g. a different laser at (g) could be used when necessary without any adjustment to the optics and gave a focussed spot in the correct place on the sample. The spot diameter of 633 nm light using a NA 0.15 objective was measured as 1.5 μm.

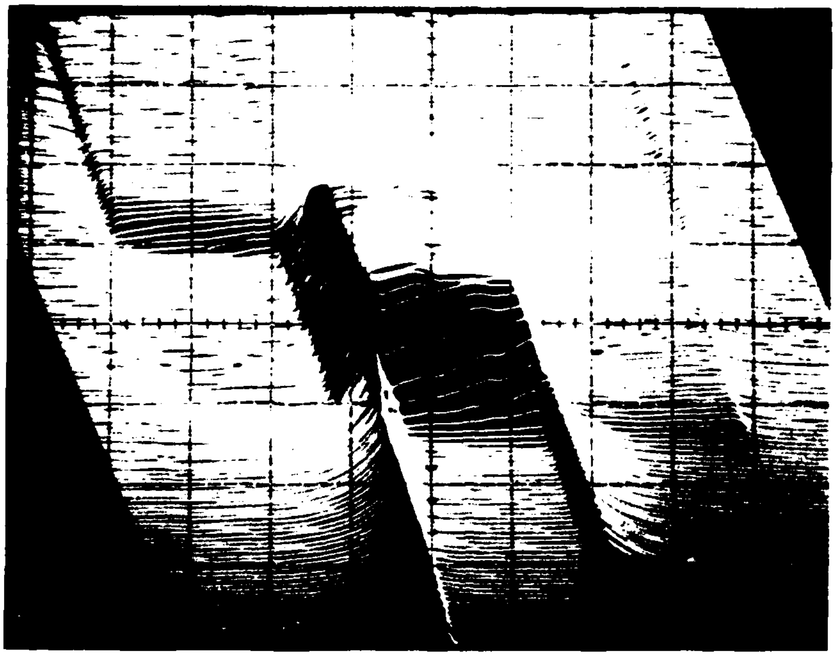

Figure 3

Responsivity map of one element of an array of 50 μm square CMT diodes (Cutoff 4.5 μm) using 633nm light

3. RESPONSIVITY MAPPING

The simplest use of the optical probe is in mapping the responsivity of a detector to visible light, usually 633 nm from a He Ne laser. Although the detectors considered here are intended for long wavelength IR (3 to 10 μm) various experiments have shown that 633 nm is a reliable substitute in thin or planar detectors, and it has a much better spatial resolution. Differences between responsivity maps at IR and 633 nm have always been caused by the known optical properties of the sample surface or substrate.

3.1 Photodiode Mapping

The current generated by a photodiode must be detected by a low impedance amplifier, and figure 3 shows the current mapped as the light spot described a raster scan over a CMT diode. In this figure a rather coarse raster was used to allow individual lines to be followed for quantitative measurement, and the current is displayed as a vertical deflection added to the raster. This diode was one of any array of 50 μm square elements.

Regions of high responsivity have been highlighted by modulating the CRT intensity by the signal, and some 'perspective' is given by adding part of the Y raster to the X deflection of the CRT. The figure demonstrates the high resolution possible with the spot scan and shows that the detector response is uniform to a few percent with no 'dead' areas. The prominent ridges in the foreground are caused by carriers generated outside, and diffusing to, an area of the p-n junction buried below the opaque contact strip. From the shape of the ridges a diffusion length of about 8 μm can be calculated. The two adjacent detector elements are visible as positive or negative responses because the substrate of these diodes has a high resistance and their response cannot be effectively earthed.

There are not usually any saturation effects in diodes so only heating limits the intensity of light used. Reference 1 discussed the non uniform maps given by diodes with high sheet resistance.

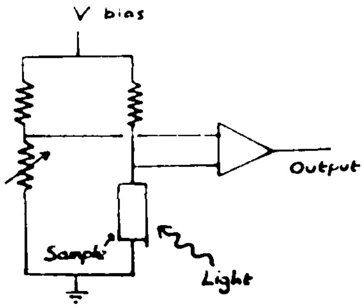

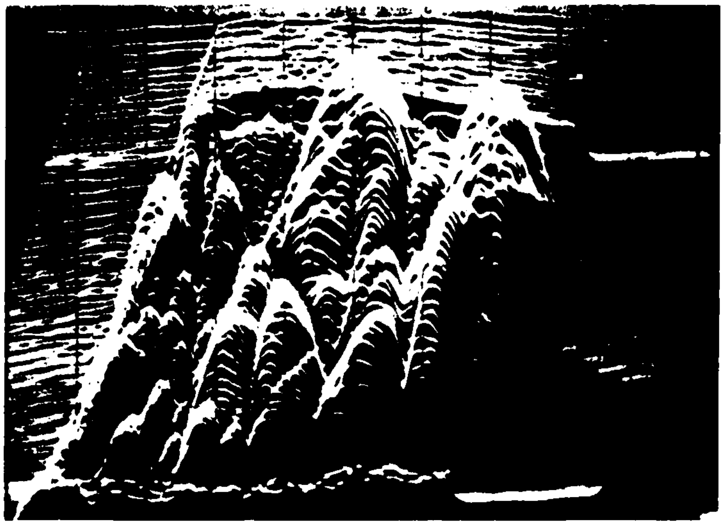

Figure 4

Responsivity map of a CMT photoconductor 500 μm square incident power 10 μw

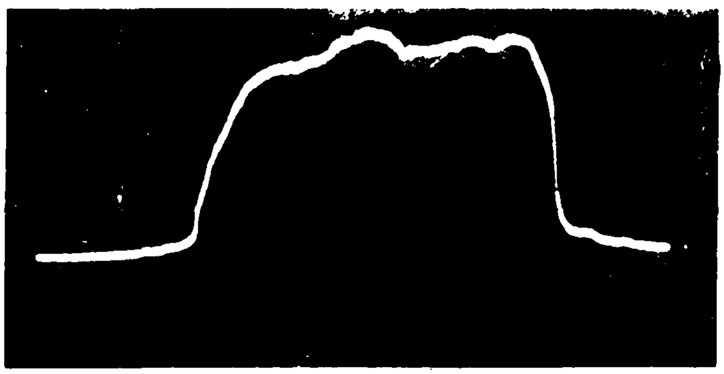

Figure 5

Responsivity linescan along a CMT 'SPRITE' detector

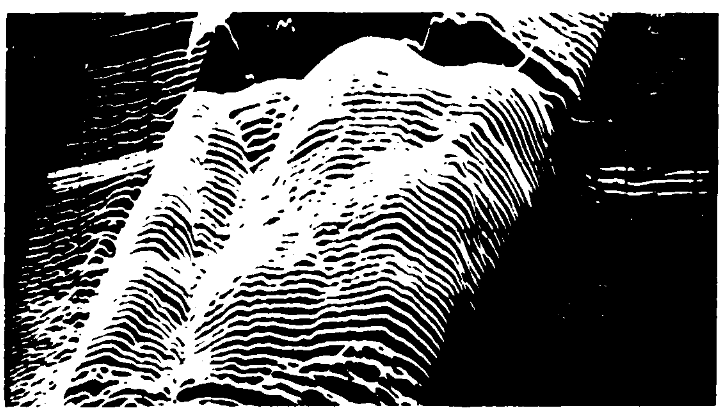

Figure 6

The photoconductor of fig 4 mapped using 150 μw of light to show the loss of resolution

3.2 Photoconductor Mapping

The light-induced change in the conductance of a photoconductor can conveniently be detected as a change in the 'balance' signal in a Wheatstone bridge (see fig 4). D C Coupling in this way allows local measurements of responsivity as well as fast scans, although much higher sensitivity can be given when a modulated light source and a phase sensitive detector are used. Small signals are sometimes tolerated because it is important to limit the incident light to a level where the photoconductor does not saturate i.e. to ensure that at all (or most) parts of a focussed spot the induced carrier concentration is much less than in the sample. Because the sample may be non uniform this level can only be found by reducing the intensity until all parts of a linescan such as fig 5 are equally reduced.

Figure 4 shows a map of the responsivity of a CMT photoconductor about 500 μm square, which has been damaged by an experimental surface coating. Because the specimen is 10 μm thick it is effectively 2-dimensional. The coating has seriously reduced the minority carrier lifetime (τ) in many regions, causing low response. A small signal from regions off the square is due to scattered light reaching the sample from its transparent substrate. The incident power is about 10 μw

When the incident power was raised to 150 μw the CMT within several diffusion lengths of the spot was saturated with carriers, and most of the detected signal was then due to the large annular region outside this. Spatial resolution was therefore much poorer. (In n-type CMT L_D is about 50 μm) See fig 6.

Some use may be made of the saturation process when finding the best focus for the spot in the absence of any sharply defined surface features. As focus is appointed the spot size is reduced, generating carriers in a smaller and more saturated region of the sample with a reduced diffusion length. The photoconductive signal is therefore reduced. After this is observed the power must be reduced.

In a photoconductor the current flow in the region of the spot is complex and depends on local variations in resistivity and lifetime. Unlike the case of the photodiode, mapping of photoconductors only gives qualitative

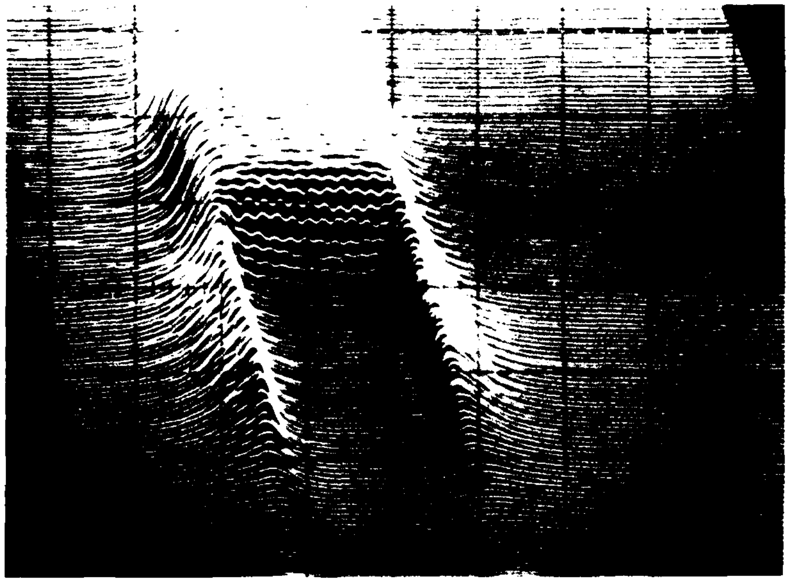

Figure 7

Responsivity map of the photodiode of fig 3, using 3.4 μm light

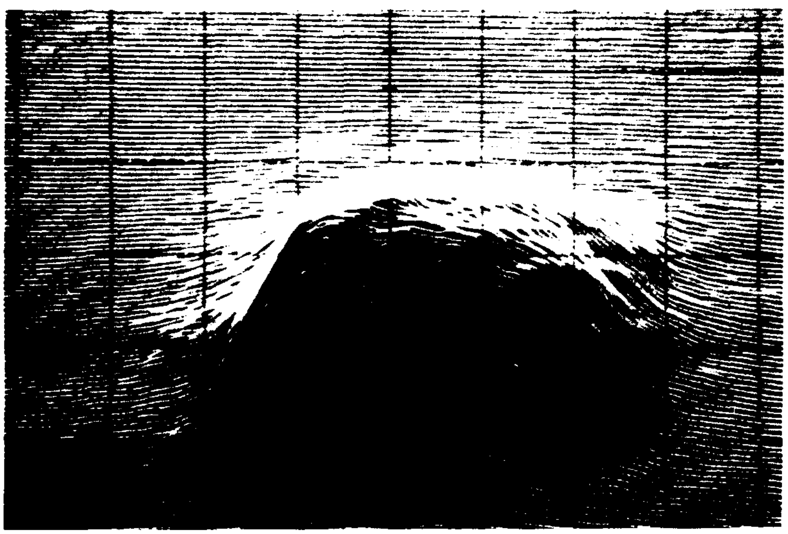

Figure 8

3.4 μm map of optically immersed detector (apparent size 180 μm 'square')

information about defects, but can be relied on if the sample is uniform, or is narrower than 2 L_D (eg the SPRITE, Ref 2).

When a thick specimen is used ($d \gg L_D$) the mapping may still be done, but since the carriers will only diffuse L_D below the surface the photoconductive signal will be small, and the depth at which material properties are sampled varies as L_D ($\propto \tau^{\frac{1}{2}}$). In the final map areas of lowest response will therefore coincide with a shallow sampling depth and may not be representative of deeper material. The technique is therefore biased towards surface defects. Longer wavelengths are needed to generate carriers below the surface.

3.3 IR Responsivity Mapping

The mapping described above has been done at longer wavelengths, both to check that 633 nm correctly represents the IR properties and detecting area of the sample, and occasionally to penetrate to a detector with a CdTe coating or a Ge lens. He Ne lasers at 1.16 μm and 3.39 μm respectively penetrate these, but the longer wavelengths require some changes in the optics of fig 1. 1.16 μm can be focussed by glass lenses and alignment can be greatly helped with a selected S1 image convertor to observe the beam

For 3.39 μm all the lenses are changed to CaF, (that transmits 633 nm for alignment,) and for high magnification a Beck reflecting objective fitted to the microscope. Although spatial resolution is worse at these wavelengths (about 5 μm) the technique has proved very useful. Fig 7 shows a map at 3.39 μm of the diode of figure 3. Note that some resolution has been lost, and that in this case (at low temperature) the crosstalk from adjacent elements is lost.

Figures 8 and 9 illustrate the use of 3.39 μm to penetrate Ge optical components. Figure 8 is a map of a 70 μm square photoconductor covered by a hemispherical immersion lens increasing its apparent size to 180 μm (with some distortion). Figure 9 was made to determine whether a SPRITE detector in a Ge-window encapsulation had rectangular or tapered elements. The tapered space between the elements is clear on both deflection - and intensity - modulated pictures, and the 'horn' readout region is also visible.

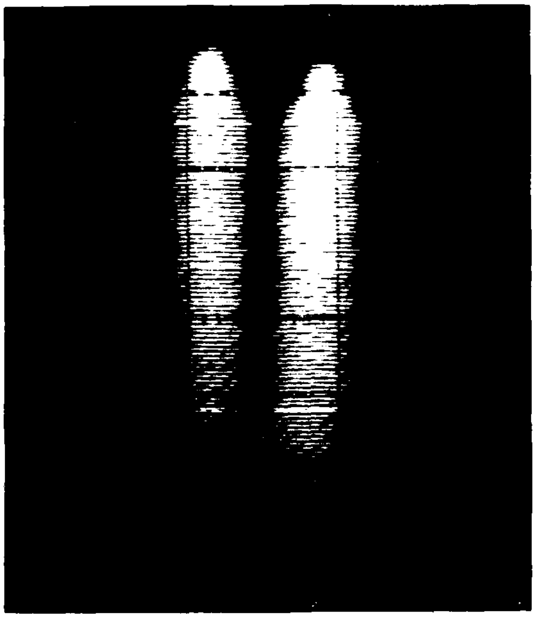

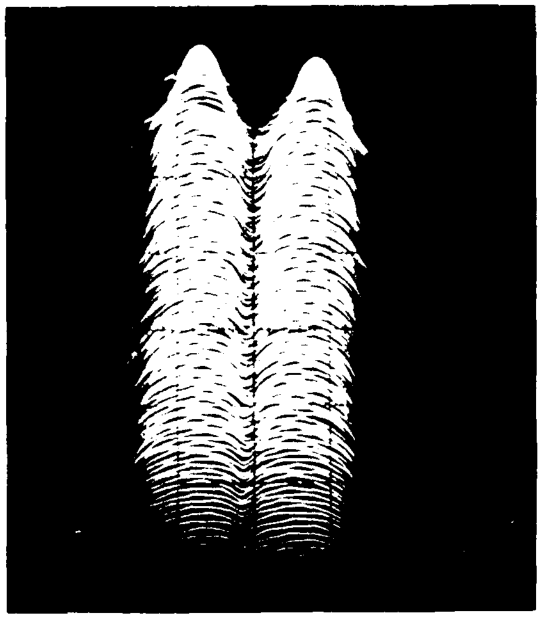

Figure 9

3.4 μm map of two 'tapered' SPRITEs in a sealed encapsulation.
a. Intensity modulation b. deflection modulation
(Device length 700 μm)

Figure 10

Reflected-light map of an array of 25 x 100 μm photodiodes (dark rectangles)

Many of the measurements described here can be carried out in a SEM but it would be unlikely to have potential as a routine assessment tool.

The optical microprobe described here is made from standard optical components and electronic instruments and has been successfully used in the investigation of many semiconductor device problems

ACKNOWLEDGEMENTS

Considerable help in setting up and operating the apparatus has been given by S E Reed, and the measurements discussed in sections 4 and 9 have been made with the assistance of L Lewell and A Walsh.

Care must be taken not to measure the decay of photocurrent by conduction through a leaky (low impedance) diode; ref 1 shows that the current detected within the area of a planar diode with sheet resistivity r and junction conductance g varies as the distance x from the contact.

$$I \propto \operatorname{sech} \sqrt{rg}\, x$$

9. DISCUSSION

This memo has described a range of measurements which have been carried out with an optical microprobe. In each of these techniques useful measurements have been made on CMT devices (Si devices and bulk samples have also been assessed at various times). The apparatus has been set up as a research tool and therefore each class of measurement requires skill in operation, but for mapping or other measurements each configuration of the apparatus could be set up and used routinely with little trouble.

Alternative methods of carrying out one or more of the measurements have been used previously. Clearly it is possible to move the specimen rather that the light spot, and this has the advantage that more complex optics can be used, and that accurate (digital) control of the spot position is possible. The disadvantage of the technique is the limited speed of scan (a raster would take minutes rather than seconds) and accommodating heavy cryostats and sample holders is difficult.

Reference 6 describes the measurement of mobility and responsivity mapping using a high speed scanning mirror. This is essential for SPRITE pulse measurements, but is much more difficult to control for the mapping described in section 3.

Lastly a SEM can be used to inject carriers in place of the light spot. This has a much higher resolution than any optical technique and is commercially available with EBIC and specimen current detection, but has the disadvantages of electrostatic charging and possible damage of a specimen, the need to operate in a vacuum with a limited access to the specimen and high cost.

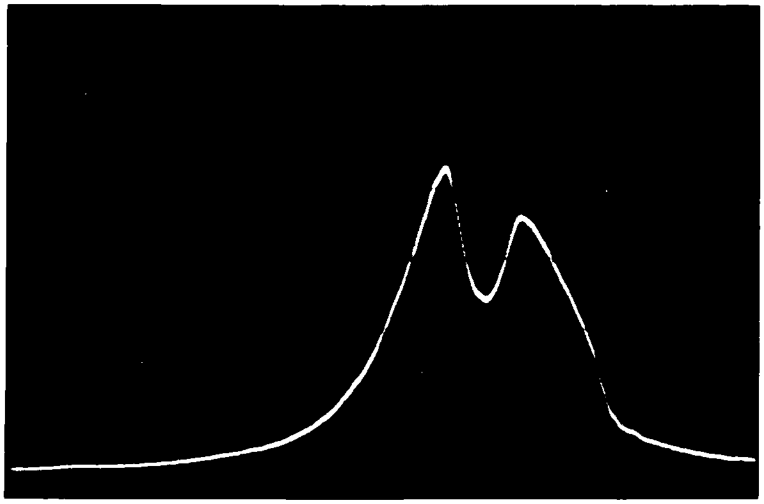

Figure 21

Responsivity Linescan of a p-type CMT sample; signal detected by an n-type diode (with central obstruction).

The left hand side of the trace gives the diffusion length (1 div = 100 μm) a contact prevents a similar trace being shown at the right.

7. PHOTOVOLTAIC DEFECT MAPPING

Measurements of the types described in sections 4 to 6 have not been successfully applied to p-type CMT because of its much lower lifetime (τ < 20ns) and higher mobility. Responsivity mapping of a photoconductor may be carried out with no difficulty, but CMT p-type samples have some features that have enabled local non uniformities to be mapped in a noval way.

Figure 19 shows photovoltage measured along the axis of two rectangular samples, and the important feature is that a photovoltage is generated with zero current bias (the centre trace) in many samples. The shape of the lines and behaviour with bias are consistent with the scan cutting a series of narrow n-type regions in a p-type matrix. Fig 20 shows raster scans of these samples with intensity modulation, and displays well the network of defects that cover the samples (about 1 mm x 0.3 mm). The defects are serious enough to affect the properties of diodes made from those regions, and this mapping technique is a useful method of non-destructive assessment. SEM induced currents can be used to detect these defects but although the SEM has high resolution, it has the disadvantage that the sample can be damaged at high beam currents (see ref 9).

8. DIFFUSION LENGTH

Section 3.1 suggested that diffusion length in diode structures could be measured from the shape of the responsivity map. This assumes that the material is uniform through its volume, so in the case of a planar p-n junction (eg fig 3) only the diffusion length outside the junction may be measured.

The technique consists of measuring the exponential decay of photocurrent with distance beyond the junction, and where L_D is long it is necessary to prepare special samples for this measurement, with a relatively large area of material, and a detection region, eg a diode, to detect the diffusing carriers. Figure 21 is a typical linescan of photocurrent made in this way on a p-type sample from Mullard Ltd; L_D is measured as 60 μm

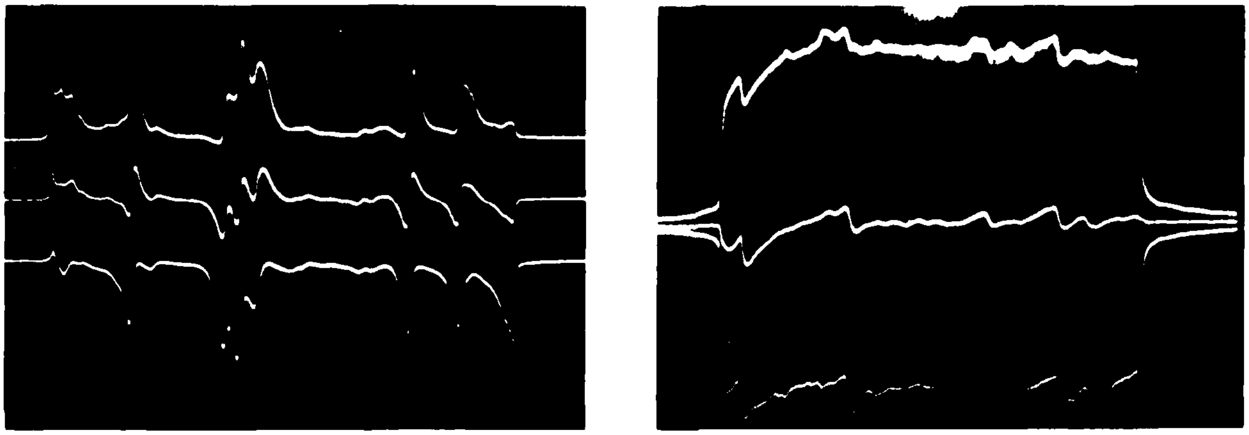

Figure 19

Linescan of photovoltaic defects in a CMT p type (Bridgman) samples upper trace positive bias, centre trace zero, lower trace negative bias.

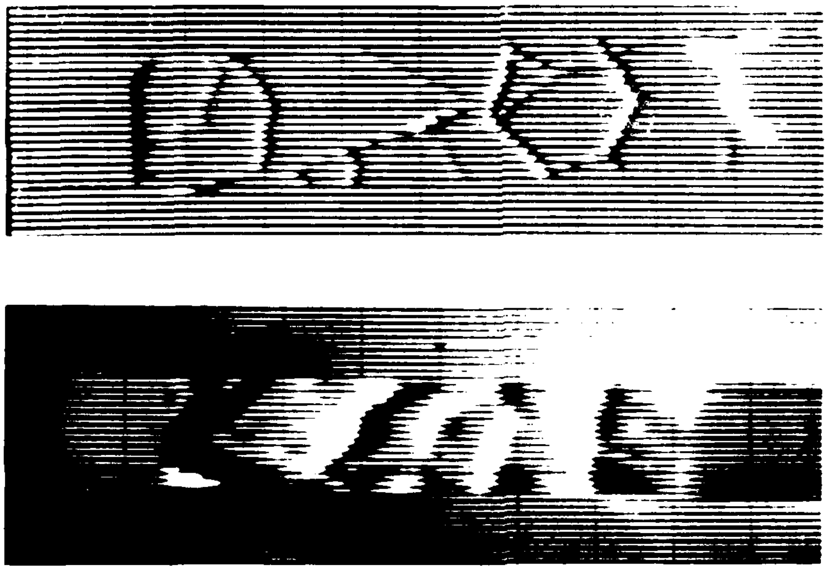

Figure 20

Map (using intensity modulation) of photovoltaic defects in the CMT samples of Figure 19 (1200 μm x 200 μm)

6. AMBIPOLAR MOBILITY

Integration of the scanned image takes place in the SPRITE detector (2) because the ambipolar mobility μ_a of photogenerated carriers is finite. A neutrally charged carrier packet can be made to drift at a velocity matching the image and it will therefore increase. Measurements of μ_a can be made by detecting the 'matched' condition using a fast scanned light spot (6) but μ_a has also been measured for n-type CMT by the optical probe in two ways. Both have given useful results and are fully described in ref 7, so they are only summarised here.

6.1 Time-of-flight

Carriers generated by a short light pulse drift towards the SPRITE readout contact at a velocity ν given by

$$\nu = \mu_a E$$

where they are detected as a voltage pulse.

A series o⁻ measurements of the drift time for different positions of the spot therefore gives μ_a as a function of position. This is Shockley-Haynes experiment (8). Fig 17 shows typical delayed pulses observed in a silicon sample with SPRITE geometry.

6.2 Integration Length

Carriers generated by a steady light source decay with a time constant τ as they drift to the readout. Plotting the voltage at the readout as a function of spot position measures the drift length L given by

$$V = V_o e^{-\frac{x}{L}} \quad \text{and} \quad L = \mu_a E\tau$$

So the technique relies on a knowledge of τ and requires it to be uniform for satisfactory results.

Fig 18 is an example of an integration length measurement.

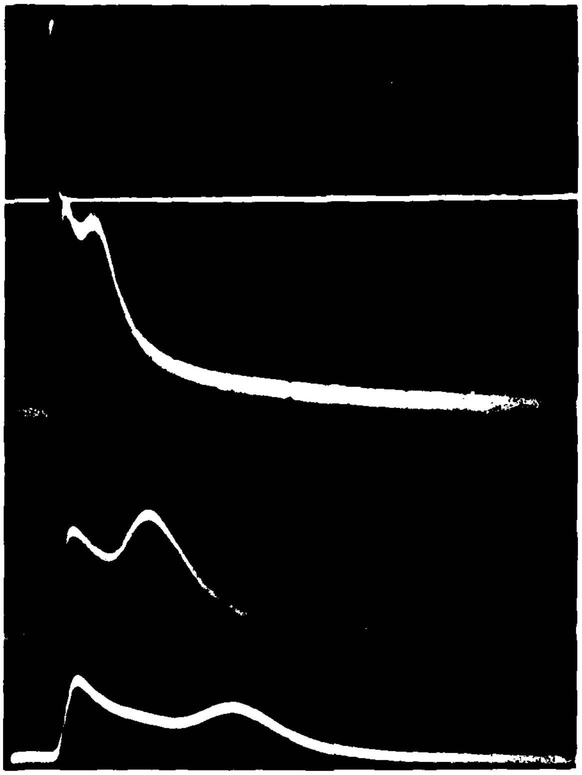

Figure 17

Time delayed secondary pulses from a 1mm SPRITE structure in silicon for increasing separation of light spot from readout.

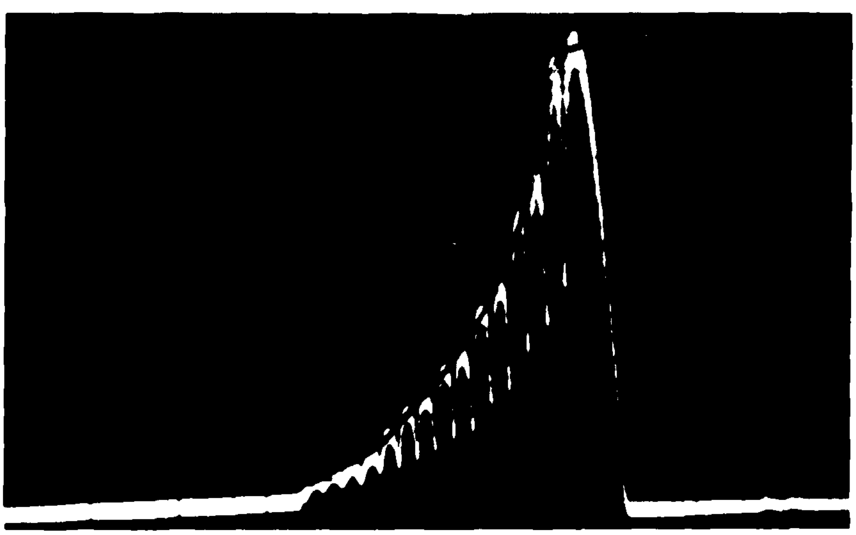

Figure 18

Meander SPITE linescan of readout signal as a function of spot position showing the exponential decay of current from regions distance x from the readout (at right).

As emphasised in section 3, in a thick sample ($d > L_D$) τ will be sampled in a region near the surface whose size varies as $\tau^{\frac{1}{2}}$ This means that areas on the surface with low τ may give a misleading impression of the values at deeper levels from where a detector may be made. The technique described here is therefore more suited to monitoring defects in thin specimens such as the SPRITE detector and its preceding stages of manufacture.

5. PHOTOLUMINESCENCF

A few measurements have been made of photoluminescence from CMT samples using the optical probe. These were attempts to show that radiative recombination took place at low excitation in CMT for the 3-5 μm IR band; this was assumed in Ref 4. Not only could the light spot be accurately positioned on a small detector, but by scanning it photoluminescence should be mapped and shown to coincide with the sample shape.

Two techniques were used. First, pulsed illumination on a sample should cause a uniform light emission (at about 4 μm) with the characteristic decay time of τ. A second detector with a smaller band gap (PbTe diode at 77k) could be used to detect any emission, but although luminescence may be observed, only the correct value of τ would confirm that radiative recombination was important at low excitations.

Secondly light transmitted by the illuminated sample (and therefore IR) should be detected by a detector sandwiched behind it. This method is more sensitive but requires the second detector to be at the same temperature as the sample.

The results of these tests showed that radiative recombination was <u>not</u> the major recombinations mechanism in CMT of even the longest τ. The first method showed that a 10 μm thick CMT sample with τ of 15 μs had a quantum efficiency of less than 10^{-3}, and the second method only detected significant photoluminescence at temperatures below 50k. Fig 16 shows a map of IR photoluminescence at 20K.

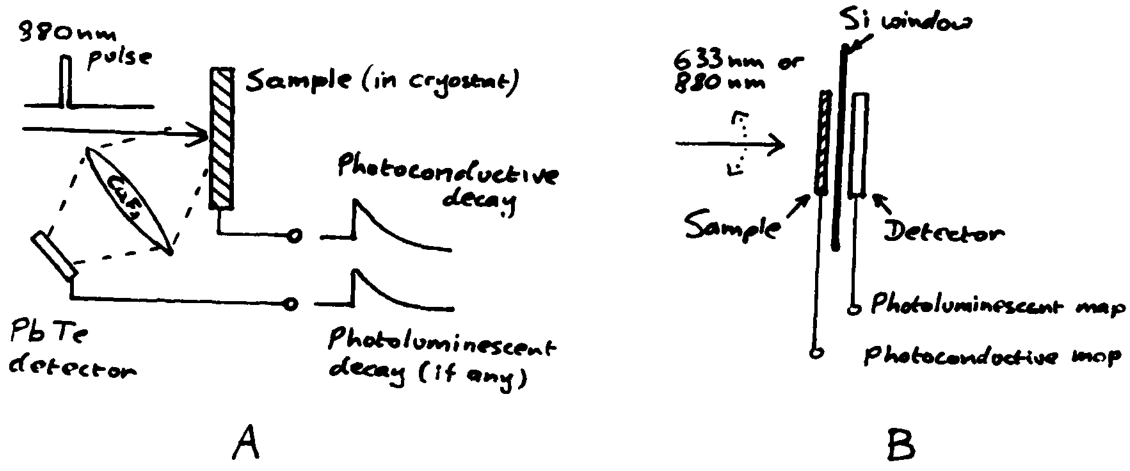

Figure 15

Photoluminescence experimental set-up

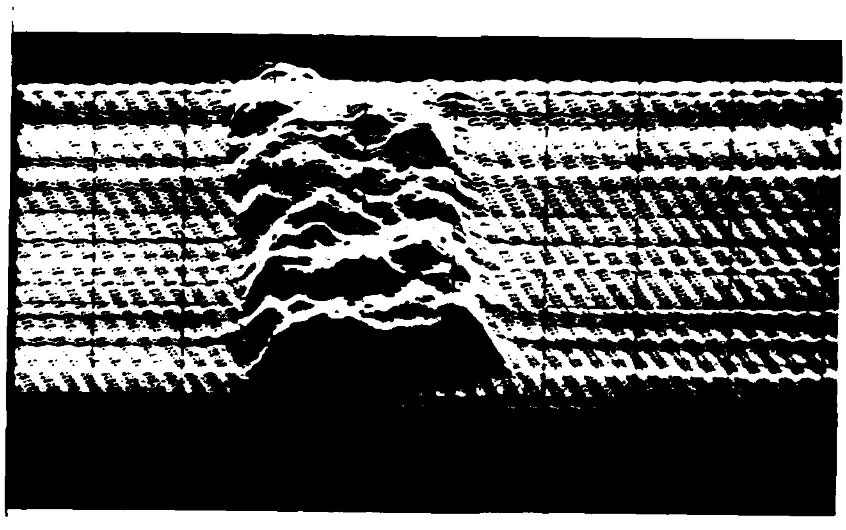

Figure 16

Map of 20K photoluminescence of CMT sample (λ < 5 μm)

as carriers diffuse outwards to occupy a larger volume of the sample. This is seen in figure 11. Sufficiently long after the light pulse the photoconductive signal has usually been exponentially decaying and it is therefore possible to define τ and display it as a function of position.

Figure 12 shows how this is done. Boxcar detectors sample the voltage pulse at two points separated by a time t_1 and subsequent analogue computing circuits convert the detected levels (V1 & V2) to a voltage proportional to τ

$$\text{i.e.} \quad \tau = t_1 \log_e \left(\frac{V1-Vo}{V2-Vo}\right)^{-1} \qquad (2)$$

A third boxcar (Vo) clamps the level before the pulse to zero to compensate for drift etc.

Figure 13 shows one use that has been made of this technique; the measuring spot has moved along the axis of a 'meander SPRITE' (3) in which notches cut from alternate sides force the bias current to move in a zigzag path. The two undulating traces are the signals from the two boxcar detectors V1 and V2, and the smooth curve is the value of τ calculated by equation 2. Note that τ is independant of the amplitude of the signals V1 and V2. This trace shows τ is about 3 µs except near the negative electrode (on the left) where minority carriers are swept out of the sample before recombining. Figure 14 shows that at low bias the sweep-out effect is not observed. Figure 14 also shows that a greater variation of τ along the specimen; this is because carriers generated at high bias sweep through local defects, averaging their effects on τ. The spatial resolution of the light source is about 7 µm.

References 4 and 5 give examples of how this technique of measuring τ has been used to investigate the surface properties of small CMT samples. Even within a sample 500 µm square it was not unusual to find variations of τ of 50 per cent, but measurements could still be made on selected areas within the sample.

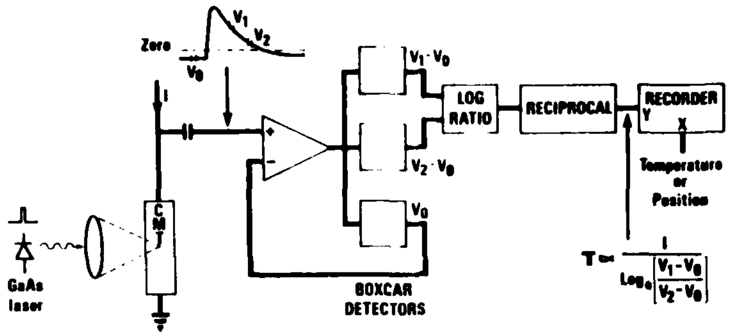

Figure 12

Diagram of the anlogue computing circuit to measure τ (see fig 2)

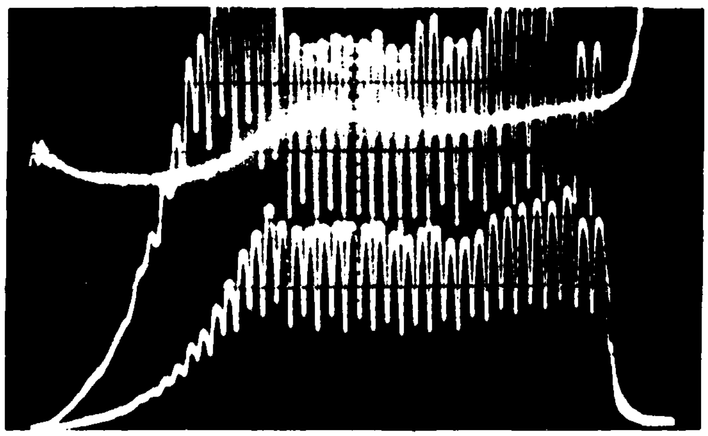

Figure 13

Plot of lifetime as a function of position in a 'meander' SPRITE
(Smooth line 1 division = 1 μs, centre zero)
Showing also the boxcar detector outputs (see fig 12)

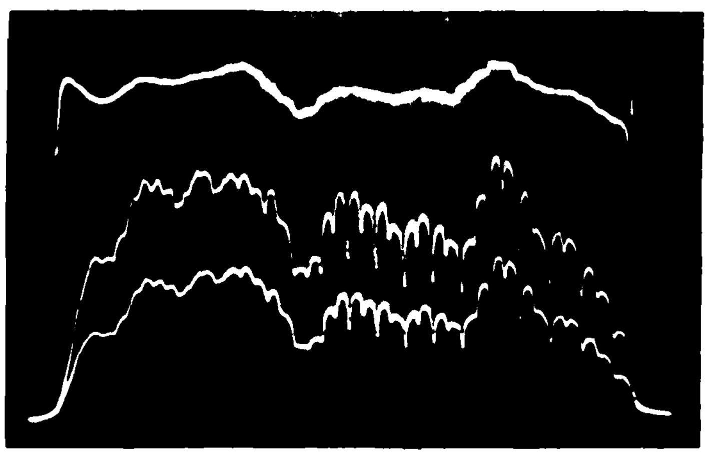

Figure 14

Lifetime of the devices of fig 13 at a low bias current

PART 2 LOCAL MEASUREMENTS OF SEMICONDUCTOR PROPERTIES

This part of the memorandum describes measurements made on small thin photoconductive devices, typically tens of microns square and 10 µm thick. A convenient sample shape in the SPRITE detector (2) to which the measurements are relevant.

4. MINORITY CARRIER LIFETIME

A standard way to measure minority carrier lifetime (τ) is to observe the time constant of decay of the conductance after a pulse of carriers has been injected by a light pulse. The scanning apparatus described above can put illumination on a small area, and a convenient pulse of light comes from a GaAs 880 nm laser whose junction is imaged on the sample. It can be driven by a standard 50 w pulse generator with little electrical interference if metal parts of the dewar etc are suitably earthed. A double heterojunction laser gives pulses typically on 500 ns long and can be used to measure lifetimes as low as 20 ns. Because the CMT samples usually measured had impedances as high as 10 kΩ the biasing and detection circuits had to be as close as possible to the sample when short lifetimes were detected. In the case of the CF204 crystat a FET amplifier was mounted at the cold end of the sample probe to drive the coaxial leads in the probe.

At any position of the light spot the exponential decay of voltage across the sample may be monitored and τ calculated.

$$V = V_O \exp \frac{-t}{\tau} \tag{1}$$

This value of τ is an average over the volume of the sample in which carries are generated (approximately L_D in radius), but even in a uniform sample of finite size the exact form of the decay curve has not been possible to calculate, since it involves a cylindrical or spherical carrier diffusion affecting the conductance of a finite sample with 2 dimensional current flow.

Saturation can increase the effective sampling volume, and one effect frequently seen is an <u>increase</u> of photoconductive signal after the light pulse,

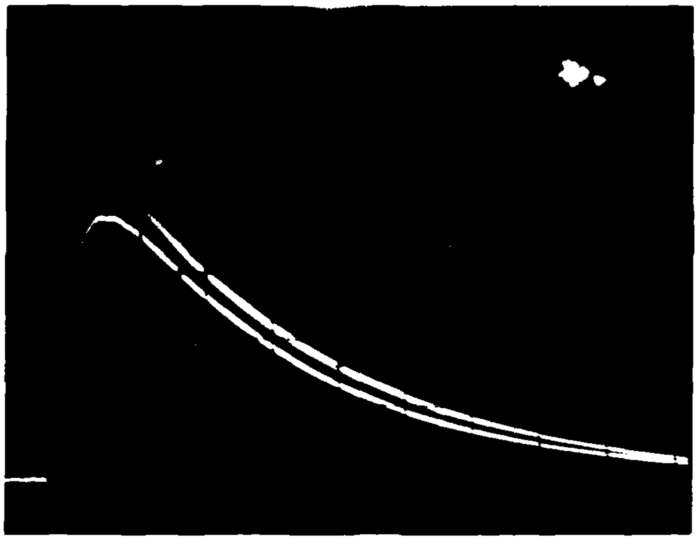

Figure 11

Photoconductive response to a short pulse of illumination - Lower trace focussed spot, upper trace defocussed. Laser pulse occurs 0.7 to 1.0 divisions from LHS ($\tau = 5.4\ \mu s$)

A waveguide CO_2 laser and Ge optics in the apparatus has allowed responsivity to be mapped at 10.6 μm, but resolution is worse than 10 μm and no useful results have been obtained at this wavelength.

3.4 Reflectivity Mapping

One further use that can be made of this apparatus is as a scanning optical microscope, in which reflected light is detected and displayed. This is done simply by a partial reflector behind the microscope objective and a detector for the appropriate wavelength. This can be used to identify devices in an array simultaneously with their responsivity mapping, and fig 10 shows some 25 x 100 μm detectors and their contacts imaged in this way.

REFERENCES

1. H A Tarry RSRE (Baldock) Technical Memorandum no 1033

2. C T Elliott et al Infrared Physics 22 31 (1982)

3. C T Elliot et al RSRE Memorandum 3144

4. H A Tarry A M White RSRE Newsletter no 5 (1981) Article 10

5. H A Tarry A M White 11th European Solid State Devices Conference 'The effect of surfaces on the minority carrier lifetime of $Cd_xHg_{1-x}Te$

6. D J Wilson Private Communication

7. S E Reed, H A Tarry RSRE Memorandum to be published

8. D E Lacklison, G Duggan J App Phys 55 4257 (1984)

9. S E Reed H A Tarry RSRE Memorandum 3746

DOCUMENT CONTROL SHEET

Overall security classification of sheet UNCLASSIFIED

(As far as possible this sheet should contain only unclassified information. If it is necessary to enter classified information, the box concerned must be marked to indicate the classification eg (R) (C) or (S))

1. DRIC Reference (if known)	2. Originator's Reference Memorandum 3745	3. Agency Reference	4. Report Security Classification UNCLASSIFIED
5. Originator's Code (if known)	6. Originator (Corporate Author) Name and Location Royal Signals and Radar Establishment		
5a. Sponsoring Agency's Code (if known)	6a. Sponsoring Agency (Contract Authority) Name and Location		

7. Title A SCANNING OPTICAL MICROPROBE FOR INFRARED DETECTOR MEASUREMENT
7a. Title in Foreign Language (in the case of translations)
7b. Presented at (for conference papers) Title, place and date of conference

8. Author 1 Surname, initials Tarry H A	9(a) Author 2	9(b) Authors 3,4...	10. Date	pp. ref.
11. Contract Number	12. Period	13. Project	14. Other Reference	

15. Distribution statement Unlimited
Descriptors (or keywords) continue on separate piece of paper

Abstract

An optical probe apparatus is described which has been used for mapping the responsivity and defects of a range of IR detectors and has been extended to measure minority carrier lifetime, ambipolar mobility, photoluminescence and diffusion length. Each use of the apparatus is illustrated with experimental results.

/4 8 =

S80/48

END

FILMED

5-85

DTIC